frontiers in Materials

ORIGINAL RESEARCH
published: 01 September 2021
doi: 10.3389/fmats.2021.739071

Hydrothermal Synthesis of Zinc-Incorporated Nano-Cluster Structure on Titanium Surface to Promote Osteogenic Differentiation of Osteoblasts and hMSCs

*Ze-hua Tang[1,2], Shan Su[1,2], Yao Liu[1,2], Wen-qing Zhu[1,2], Song-mei Zhang[3] and Jing Qiu[1,2,4]**

[1]Department of Oral Implantology, Affiliated Stomatological Hospital of Nanjing Medical University, Nanjing, China, [2]Jiangsu Province Key Laboratory of Oral Diseases, Nanjing, China, [3]Department of General Dentistry, Eastman Institute for Oral Health, University of Rochester, Rochester, NY, United States, [4]Jiangsu Province Engineering Research Center of Stomatological Translational Medicine, Nanjing, China

In this study, a novel modification strategy was established to synthesize a zinc-incorporated nano-cluster structure on titanium surface in a two-step hydrothermal reaction, and the osteogenic differentiation of osteoblasts and human bone marrow mesenchymal cells (hMSCs) was studied in the presence of this synthesized nanostructure. Analyses of the surface topography and elemental composition revealed that the zinc-containing cluster-like nanostructure was successfully prepared on the titanium surface. By altering the reaction time, three surface modifications were established. The three modified titanium surfaces had improved hydrophilicity and could continuously release zinc ions in a controlled manner. *In vitro* study displayed that three modified titanium surfaces, especially the samples prepared by reacting for 15 min, exhibited enhanced cell adhesion, proliferation, and osteogenic differentiation compared to the pure titanium surface. The study therefore conclude that the zinc-incorporated nano-cluster modification of titanium surface through a simple procedure can establish an enhanced osteogenic microenvironment and exhibit a potential strategy of titanium surface modification to accelerate the dental implant osseointegration.

Keywords: zinc, nano-cluster, titanium surface modification, osteoblast, HMSCs

OPEN ACCESS

Edited by:
Bo Yu,
Huazhong University of Science and Technology, China

Reviewed by:
Stefania Cantore,
City Unity College Athens, Greece
Yinghua Li,
Guangzhou Medical University, China
Thorsten Steinberg,
University Medical Center, Germany
Roman Matejka,
Czech Technical University in Prague, Czechia
Helena Bacha Lopes,
University of São Paulo, Brazil
Pengtao You,
Hubei University of Chinese Medicine, China

****Correspondence:***
Jing Qiu
qiujing@njmu.edu.cn

Specialty section:
This article was submitted to Biomaterials, a section of the journal Frontiers in Materials

Received: *10 July 2021*
Accepted: *16 August 2021*
Published: *01 September 2021*

Citation:
Tang Z-h, Su S, Liu Y, Zhu W-q, Zhang S-m and Qiu J (2021) Hydrothermal Synthesis of Zinc-Incorporated Nano-Cluster Structure on Titanium Surface to Promote Osteogenic Differentiation of Osteoblasts and hMSCs. Front. Mater. 8:739071. doi: 10.3389/fmats.2021.739071

INTRODUCTION

Titanium and its alloys have been widely used in orthopedics and stomatology as bone fixation devices and implants due to their excellent mechanical properties, biocompatibility, and satisfactory osseointegration potential (Alghamdi and Jansen, 2020). Although titanium implants have achieved high success rates above 90% (Lini et al., 2019), patients are still beset by the occasionally failure and long process of osteointegration mainly attributed to the bioinertia of traditional dental implants (Wang et al., 2018). Therefore, it is essential to improve the bioactivity of titanium-based materials and accelerate osseointegration. Methods for implant surface modification include roughening the surface topography at the nanoscale or microscale level, improving surface hydrophilicity, coating of the bioactive molecules and incorporating trace elements (Xue et al., 2020).

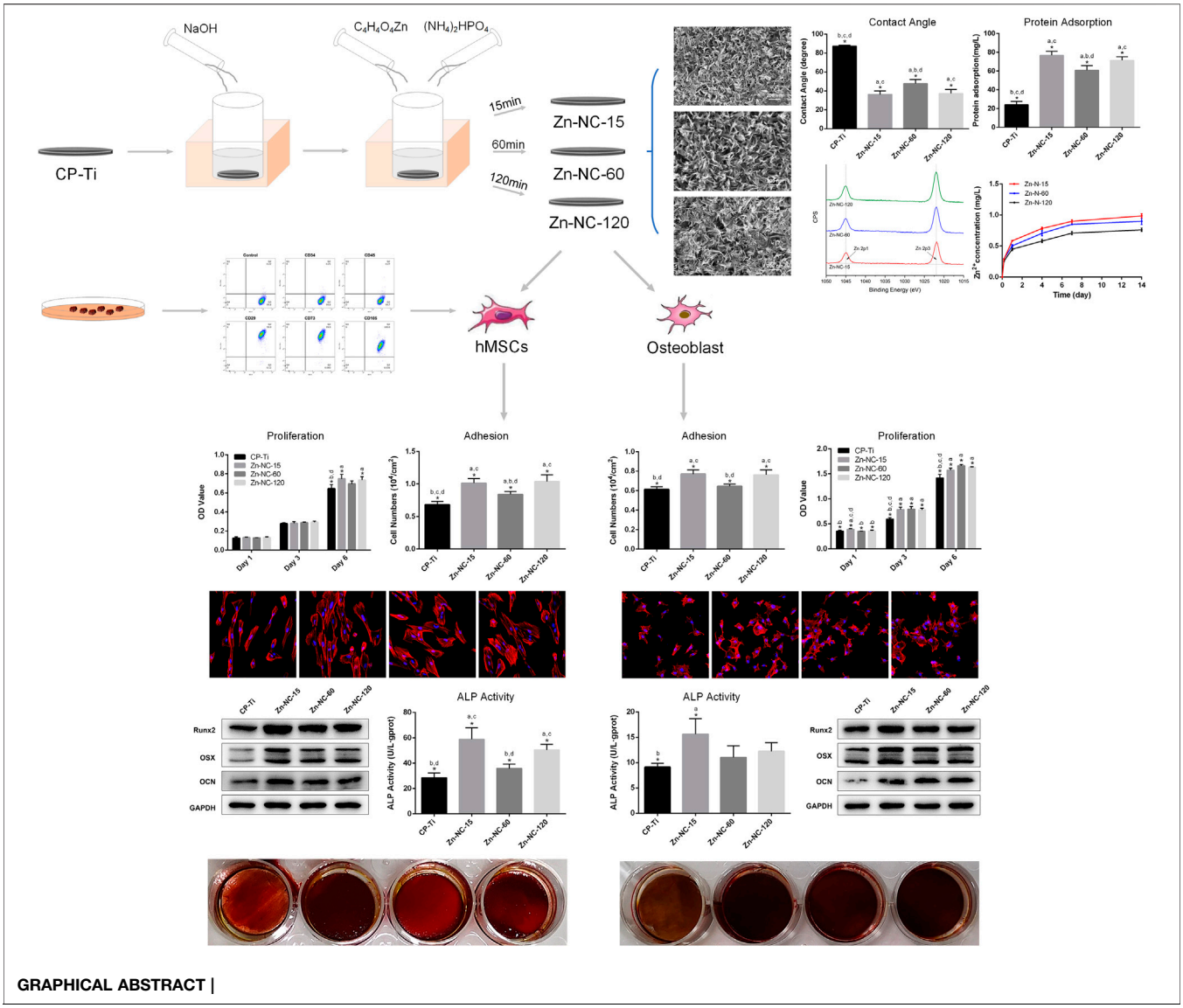

GRAPHICAL ABSTRACT |

Roughened implants can improve long-term mechanical stability and accelerate bone formation (Heberer et al., 2011; Buser et al., 2012). Surface treatments used for increasing surface roughness including grit-blasting, acid-etching, alkali heat treatment, plasma-spraying or anodization, most of which have been commercialized and proven to be clinically effective (Le Guéhennec et al., 2007). Alkali heat treatment after acid etching is commonly employed to form modified nanoscale or microscale roughened surfaces to promote biochemical bonding at the bone-implant interface and induce bone formation (Alvarez et al., 2010). Nanoscale surface roughness enhances the adsorption of proteins, adhesion of osteoblasts, and osteogenic differentiation *in vitro* and osseointegration *in vivo* (Brett et al., 2004). In addition, the nanostructure topography regulates the differentiation of stem cells. Titania nanotube formation has been demonstrated to stimulate the osteogenic differentiation of hMSCs, and the extent of stimulation could be adjusted by modifying the nanotube dimension (Li et al., 2020).

Zinc is an essential trace element that can promote cell proliferation and bone development. It directly influences osteoblastic differentiation and immune microenvironment and acts as a signal molecule in several intracellular signaling pathways (Yamaguchi, 2010). While dietary zinc deficiency interferes with normal bone growth by downregulating the expression of osteoblast marker genes, alkaline phosphatase activity, and calcium deposition (Hie et al., 2011; Guo et al., 2012). Previous studies have reported the synthesis of zinc-modified titanium by alkali treatment of the $[Zn(OH)_4]^{2-}$ complex for 24 h (Yusa et al., 2016a). Other studies have described the preparation of zinc-containing nanowires modified titanium surfaces by acid etching and alkali heat treatment in a $ZnSO_4$ aqueous solution (Shao et al., 2020). However, these preparation methods are relatively complicated and lengthy. Zinc ions released from the surface of zinc-modified titanium can stimulate the proliferation of bone marrow

mesenchymal cells by significantly influencing the expression of osteogenic marker genes and calcium deposition (Yusa et al., 2016b).

Herein, a novel procedure was established to synthesize a zinc-incorporated cluster-like nanostructure on titanium surface without using hydrofluoric acid etching or heat treatment. The modification process was straightforward and achieved synchronous completion of nanostructure modification and zinc incorporation through two simple steps of hydrothermal method at a low cost. The novel modified titanium surfaces were evaluated for their physical properties and ability to promote the osteogenesis of osteoblasts and hMSCs. We wished that this novel preparation could provide valuable references for studies aimed at cell-nanostructure interactions and surface modification designs of implants.

MATERIALS AND METHODS

Specimen Preparation

Pure titanium (99.5 wt% purity, Baoji Taiye, China) disks were used as the control group (CP-Ti) after polishing. To prepare the zinc-incorporated nano-cluster modified titanium surfaces (Zn-NC-Ti), CP-Ti was first alkalized with 10% sodium hydroxide aqueous solution in a water bath at 70°C for 15 min and ultrasonically washed with alcohol and distilled water. Subsequently, these samples were immersed in a 3:2 solution of 0.1 mol/L zinc acetate and 0.1 mol/L diammonium hydrogen phosphate in a water bath at 80°C for different periods: 15 min, 1 h, and 2 h. After ultrasonic cleaning and drying, the obtained specimens were denoted as Zn-NC-15, Zn-NC-60, and Zn-NC-120, respectively.

Surface Characterization

The surface morphology of the different samples was observed by scanning electron microscopy (SEM, ULTRA 55, ZEISS, Germany). X-ray photoelectron spectroscopy (XPS, Thermo Scientific Escalab 250Xi, United States) was used to identify the surface constituents and the bonding states. The wettability of the different surfaces was determined in triplicate using a standard optical contact angle meter (SL200B, KONO, United States).

Zinc Ion Release Assay

Newly prepared samples were soaked in 24-well plates with 1 ml phosphate-buffered saline (PBS) per well for 4 h, 1, 4, 7, and 14 days at 37°C. Cumulative concentrations of zinc ions released into PBS were quantified in triplicate using inductively-coupled plasma mass spectrometry (Agilent ICP-MS7700, United States).

Protein Adsorption Assay

To assay the protein adsorption of the samples, 150 μl minimum essential medium alpha (αMEM; Gibco, CA, United States) containing 10% fetal bovine serum (FBS, Gibco, United States) was added onto the samples and incubated at 37°C for 24 h. Next, the samples were transferred into a new 96-well plate, and 150 μl 1% SDS (Beyotime, China) was added to transfer the protein adsorbed on the samples into the solution. The amount of protein in the solution was measured using a BCA protein assay kit (KeyGEN BioTECH, China). Three samples per group were used for this assay.

Cell Culture

The osteoblast-like cell line MC3T3-E1 (OBs) was obtained from the Chinese Academy of Sciences Cell Bank (Shanghai, China). HMSCs were separated by adherence method from crushed alveolar bone brought out by the tapping drill during implant surgery in a healthy individual without systemic diseases at Jiangsu Stomatological Hospital. Both cells were grown in αMEM supplemented with 10% FBS and 1% penicillin/streptomycin (Gibco, United States), and incubated at 37°C in a humidified atmosphere of 5% CO_2. The culture medium was refreshed every 3 days and the cells were passaged at 80% confluence.

For the characterization of hMSCs, flow cytometry was performed to detect specific cell surface antigens. Cells were washed with PBS and detached with 0.25% trypsin/EDTA (Gibco, United States). The cell suspension containing 3×10^5 cells was incubated with 5 μl phycoerythrin-conjugated antimouse CD29, CD34, CD45, CD73, and CD105 (Biolegend, United States) for 30 min at 4°C. After washing twice in PBS, the cells were resuspended in PBS and passed through a flow cytometer (FACSVerse, BD, United States). The subsequent experiments were conducted with the cells after 2–6 passages.

For the induction of osteogenic differentiation, cells were cultured in complete medium as above until 70% confluence and then replaced with an osteoblast -inducing conditional medium composed of αMEM containing 10% FBS, 1% penicillin/streptomycin, 10 mmol/L sodium β-glycerophosphate (Sigma, United States), 50 μg/ml ascorbic acid (Sigma, United States), and 0.1 μmol/L dexamethasone (Sigma, United States).

Cell Adhesion and Spreading Assay

OBs and hMSCs (5×10^3 cells per well) were seeded on the different sample surfaces in 96-well plates. For the analysis of cell adhesion, cell nuclei were stained with 4′,6′-diamidino-2-phenylindole (DAPI, Beyotime, Shanghai, China) for 2 min and counted after 1 h. After OBs being cultured for 8 h and hMSCs being cultured for 24 h, each sample was fixed and stained with rhodamine phalloidin (Cytoskeleton, United States) at room temperature in the dark for 30 min and then stained with DAPI (Beyotime) for 2 min. The cell adhesion and spreading were observed using a laser scanning confocal microscope (LSCM710, Zeiss, GER). All tests were conducted in triplicate.

Cell Proliferation Assay

For the cell proliferation assay, OBs and hMSCs were seeded (2×10^3 cells/well) onto four materials in 96-well plates for 1, 3 and 6 days. Subsequently, the medium was replaced with 100 μl fresh medium supplemented with 10 μl CCK-8 reagent (Beyotime), followed by incubation at 37°C for another 2 h. After that, the incubated solution was transferred into a new 96-well plate, and the absorbance was recorded using a microplate

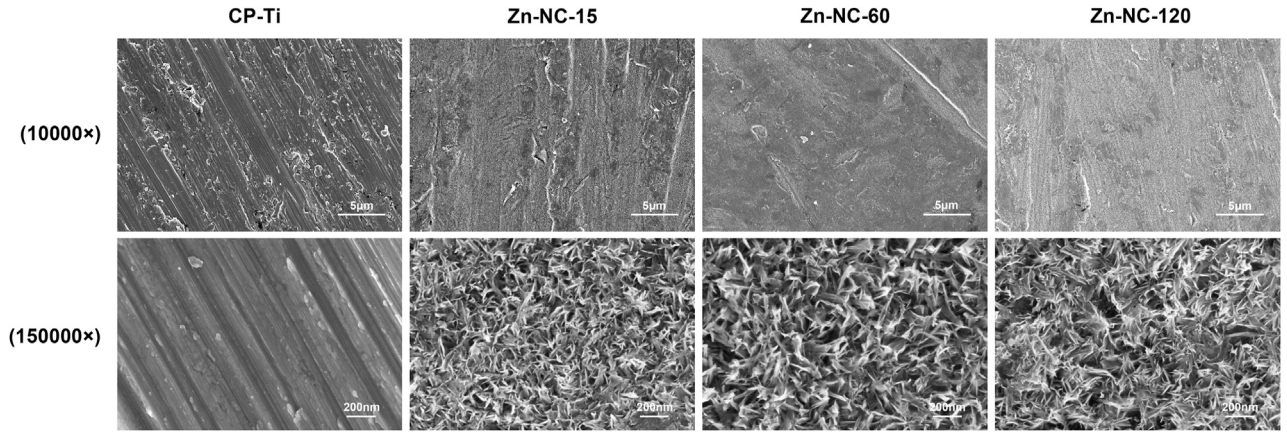

FIGURE 1 | Scanning electron microscopy images of the surface morphology of the different synthesized surfaces. Upper panel: ×10,000 magnification; lower panel: ×1,50,000 magnification.

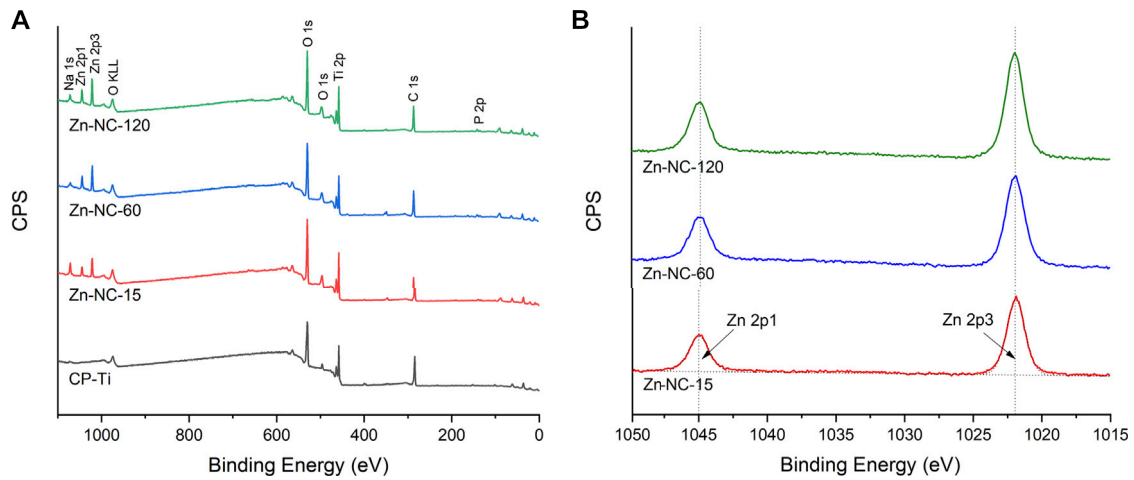

FIGURE 2 | X-ray photoelectron spectroscopy analysis of the different synthesized surfaces: **(A)** Survey spectra of the four surfaces; **(B)** High-resolution spectra of Zn 2p on the three Zn-NC-Ti surfaces.

spectrophotometer (Spectramax 190, CA, United States) at 450 nm. Three samples per group were used for this assay.

Alkaline Phosphatase Activity

OBs and hMSCs (2×10^5 cells per well) were initially plated on the four samples in a 6-well plate. After 7 days of osteogenic induction, cells from different samples were extracted using RIPA (LEA-GENE, Beijing, China) at 4°C for 30 min. The lysates were centrifuged at 12,000 rpm at 4°C for 10 min to remove cellular debris and nuclei, and then the liquid supernatants were collected. ALP activity was analyzed using an ALP assay kit (Nanjing Jian Cheng, China) and total protein content was measured using a BCA protein assay kit (KeyGEN BioTECH, China). ALP activity relative to the control was calculated after normalization to the total protein content. Three samples per group were used for this assay.

Western Blot Analysis

OBs and hMSCs (2×10^5 cells/well) were seeded onto four samples in 6-well plates. After 7 days of osteogenic induction, protein samples were extracted from the cells using RIPA and subjected to SDS-PAGE. The protein blots were then transferred to PVDF membranes (Millipore, MA, United States) followed by blocking with 5% non-fat milk for 2 h. The blots were then incubated with primary antibodies against Runx2 (12556, CST, United States), Osterix (ab209484, Abcam, United States), OCN (ab10911, EMD Millipore, United States), and GAPDH (60004, Proteintech, United States) overnight at 4°C. After washing with TBS-Tween buffer thrice, membranes were incubated for 2 h with appropriate secondary antibodies (ZB-2301, goat antirabbit IgG; ZSGB-BIO, Beijing, China; AP124P, goat antimouse IgG; Millipore) and then visualized by ECL Western Blot Kit (Millipore, CA, United States). GAPDH was used as an internal control.

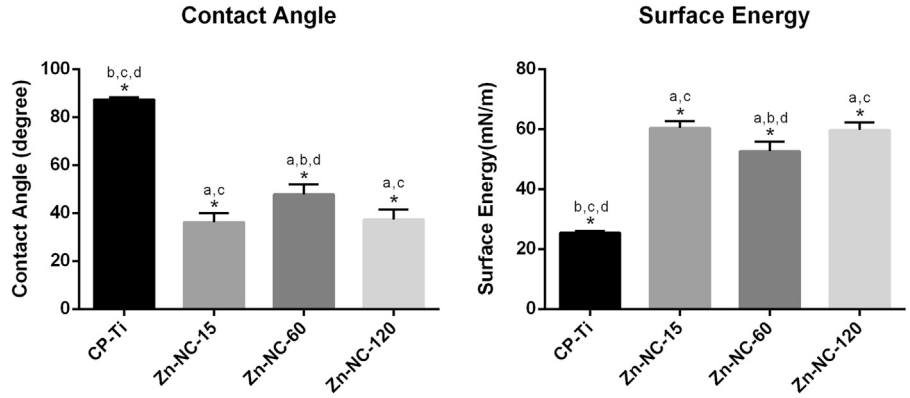

FIGURE 3 | Contact angles and surface energy of Cp-Ti and Zn-NC-Ti surfaces (n = 3). *$p < 0.05$; [a]P < 0.05 vs. CP-Ti; [b]P < 0.05 vs. Zn-NC-15; [c]P < 0.05 vs. Zn-NC-60; [d]P < 0.05 vs. Zn-NC-120.

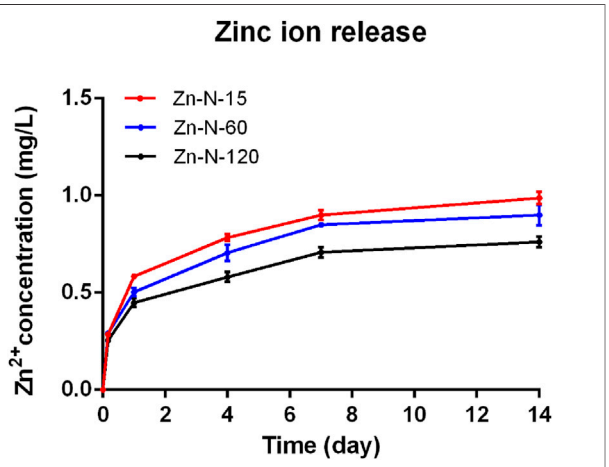

FIGURE 4 | Concentration of zinc ion released from Zn-NC-Ti surfaces into PBS after 10 min, 1 h, 4 h, 1, 4, and 7 days (n = 3).

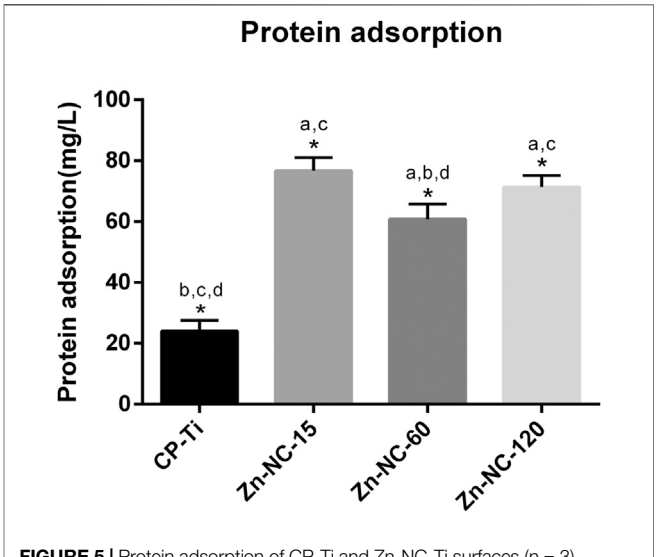

FIGURE 5 | Protein adsorption of CP-Ti and Zn-NC-Ti surfaces (n = 3). *$p < 0.05$; [a]P < 0.05 vs. CP-Ti; [b]P < 0.05 vs. Zn-NC-15; [c]P < 0.05 vs. Zn-NC-60; [d]P < 0.05 vs. Zn-NC-120.

Alizarin Red S Staining

OBs and hMSCs (2×10^5 cells/well) were seeded on four samples in 6-well plates. After 21 days of osteogenic induction, the samples were washed with PBS, fixed for 30 min with 4% paraformaldehyde, and washed with ddH_2O. Then, 1 ml of Alizarin Red S (ARS) staining reagent (Leagene, Beijing, China) was added to each well, and the reaction was terminated after 5 min with ddH_2O. The staining results of matrix mineralization were recorded photographically.

Statistical Analysis

The results were analyzed using SPSS (SPSS, Inc., IL, United States) with one-way analysis of variance, followed by the Student-Newman-Keuls post hoc test. *$p < 0.05$ indicated statistical significance.

Ethics Statement

The experiments involving human participants were reviewed and approved by the Ethics Committee of Jiangsu Stomatological Hospital (Reference number: PJ 2021-003-01; see **Supplementary Material**). The patients provided their written informed consent to participate in this study (see **Supplementary Material**).

RESULTS

Characterization of Zinc-Incorporated Nano-Cluster Modified Titanium Surface

SEM analysis of the samples (**Figure 1**) showed that the unmodified titanium surface is relatively smooth, with scratches mainly produced in the grinding step. While all modified surfaces appeared uniformly rough, overlapped and entangled cluster-like nanostructures could be observed on the Zn-NC-Ti surfaces under higher magnification. All three

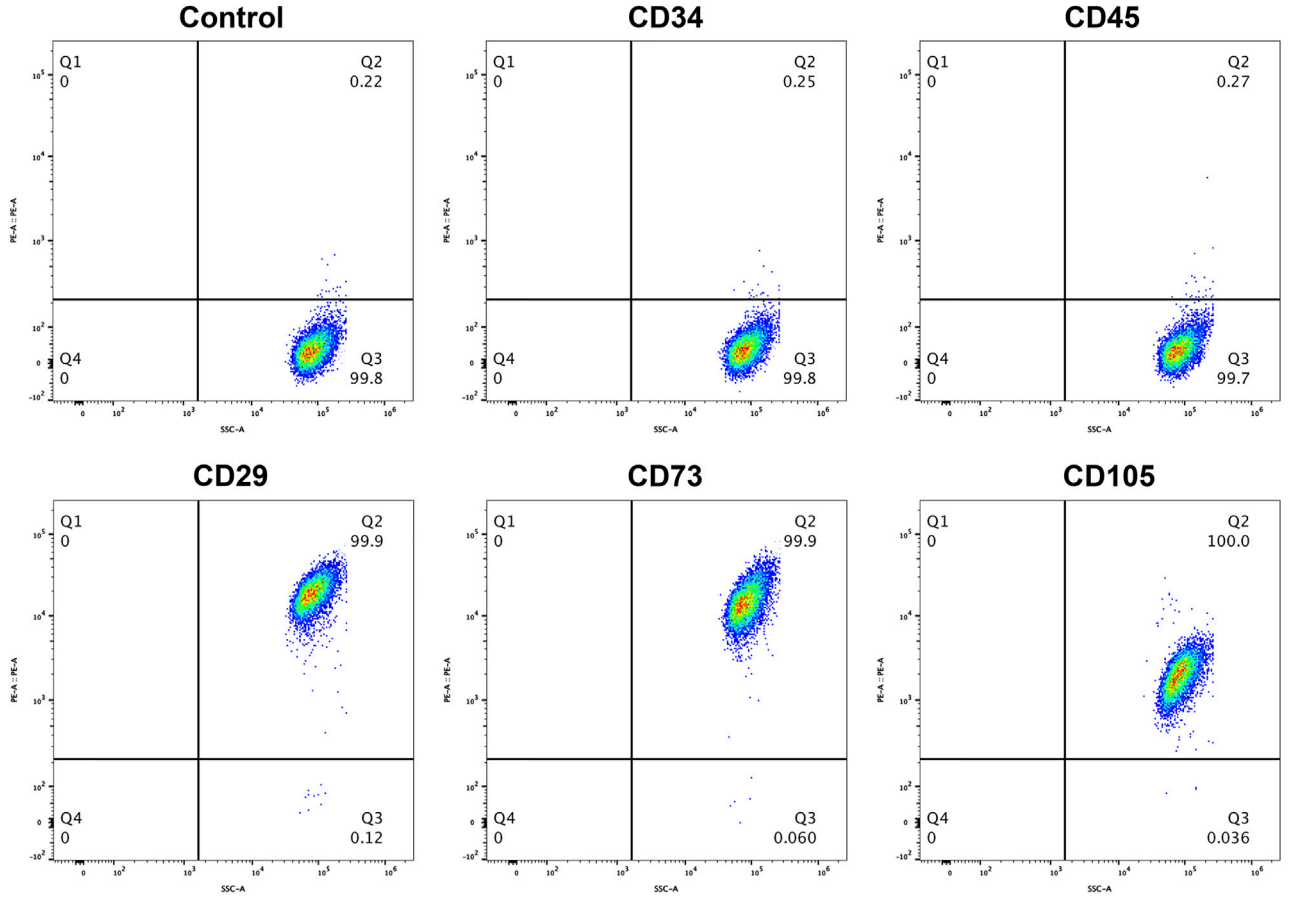

FIGURE 6 | Characterization and flow cytometric analysis of hMSCs.

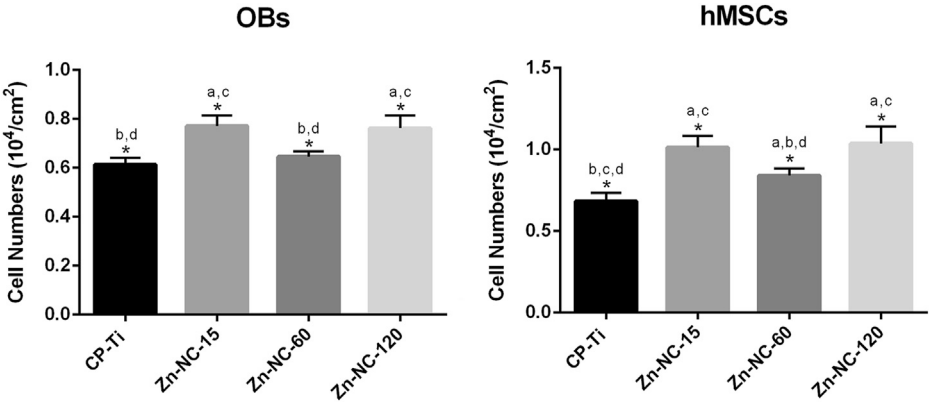

FIGURE 7 | Adhesion of OBs and hMSCs on the different surfaces analyzed by counting the DAPI-stained nuclei after 1 h of incubation (n = 3). *$p < 0.05$; $^{a}P < 0.05$ vs. CP-Ti; $^{b}P < 0.05$ vs. Zn-NC-15; $^{c}P < 0.05$ vs. Zn-NC-60; $^{d}P < 0.05$ vs. Zn-NC-120.

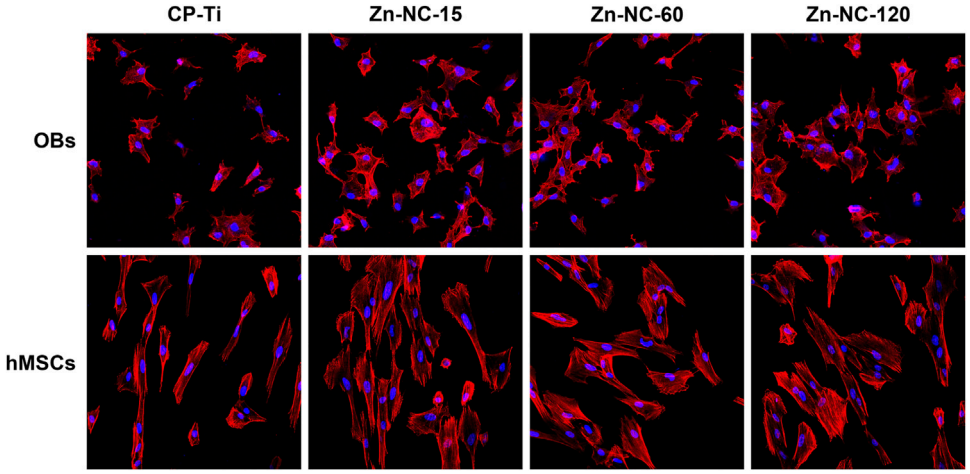

FIGURE 8 | LSCM images of OBs cultured for 8 h and hMSCs cultured for 24 h on the different surfaces at ×200 magnification.

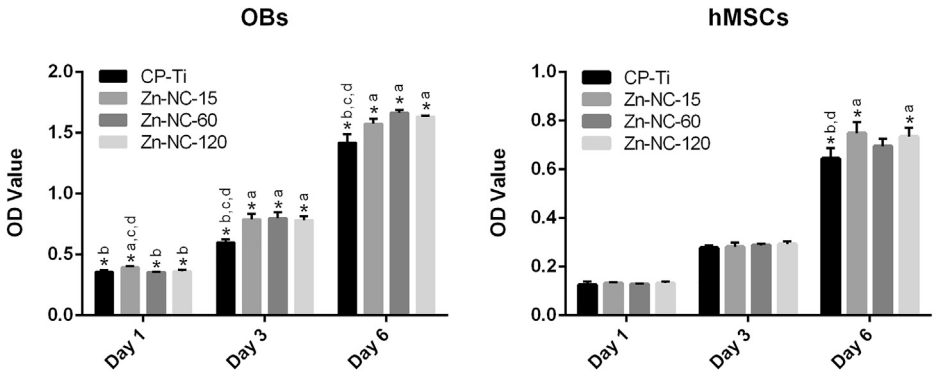

FIGURE 9 | Proliferation of OBs and hMSCs cultured for 1, 3, and 6 days on different surfaces (n = 3). *$p < 0.05$; $^{a}P < 0.05$ vs. CP-Ti; $^{b}P < 0.05$ vs. Zn-NC-15; $^{c}P < 0.05$ vs. Zn-NC-60; $^{d}P < 0.05$ vs. Zn-NC-120.

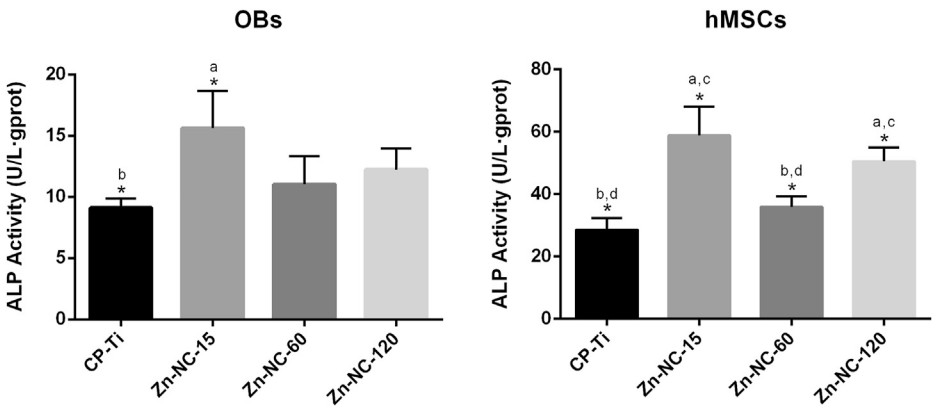

FIGURE 10 | The ALP activity of the OBs and hMSCs cultured for 7 days on the different samples (n = 3). *$p < 0.05$; $^{a}P < 0.05$ vs. CP-Ti; $^{b}P < 0.05$ vs. Zn-NC-15; $^{c}P < 0.05$ vs. Zn-NC-60; $^{d}P < 0.05$ vs. Zn-NC-120.

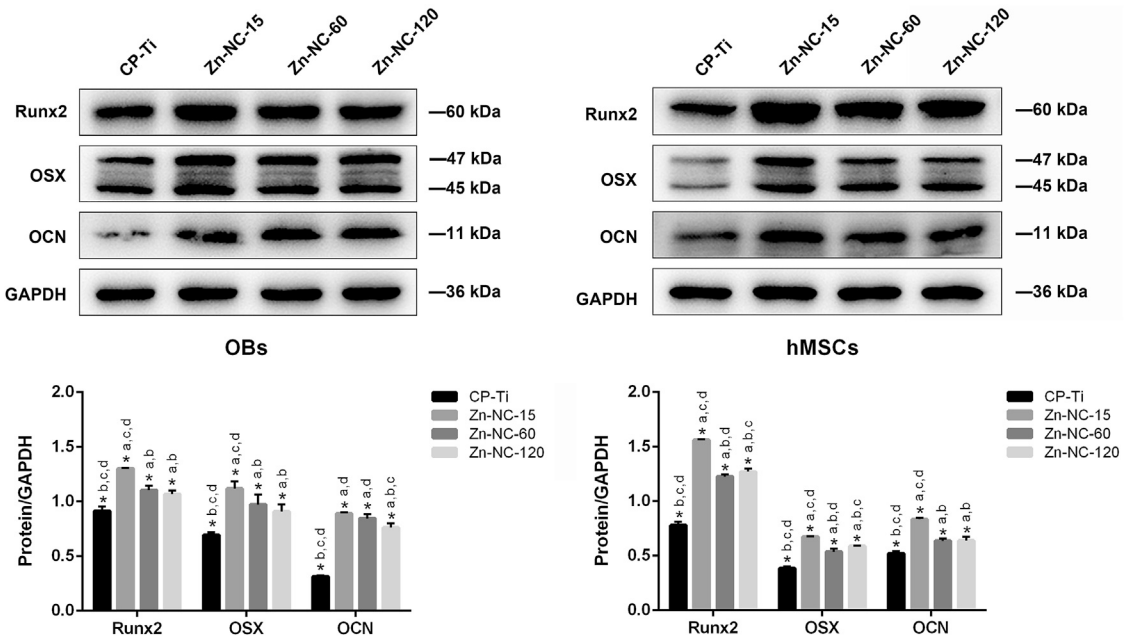

FIGURE 11 | Expression of osteogenesis-related proteins, Runx2, OSX, and OCN, in OBs and hMSCs cultured for 7 days on the different surfaces (n = 3). *p < 0.05; [a]P < 0.05 vs. CP-Ti; [b]P < 0.05 vs. Zn-NC-15; [c]P < 0.05 vs. Zn-NC-60; [d]P < 0.05 vs. Zn-NC-120.

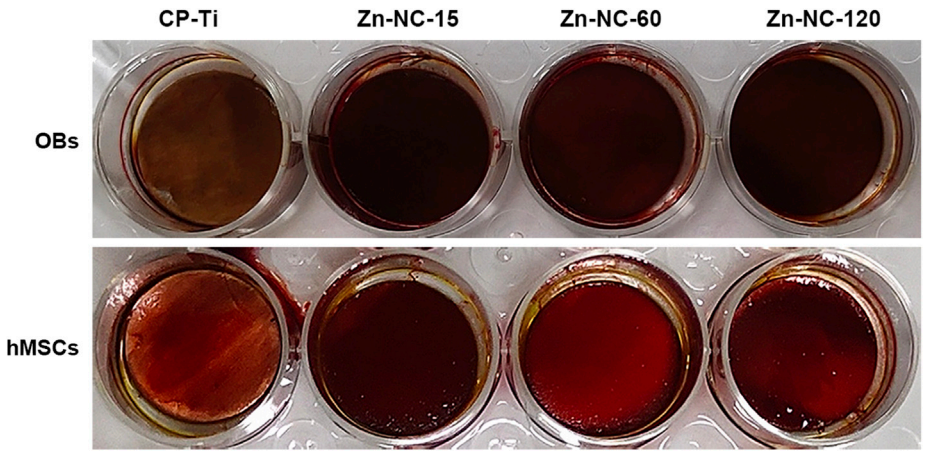

FIGURE 12 | ECM mineralization of OBs and hMSCs cultured for 21 days on the different surfaces.

modified samples (synthesized by varying the reaction time) showed similar nanotopography with differences only at the nanostructure scale. The Zn-NC-15 group exhibited the smallest nanoscale.

In the XPS analysis of the elemental composition of the samples, the wide scan spectrum (**Figure 2A**) showed that all samples mainly contained titanium, oxygen, and carbon. Zinc peaks were found in all Zn-NC-Ti surfaces but not in the control pure titanium surface, further verifying the successful incorporation of zinc into the modified titanium surfaces. The high-resolution spectra (**Figure 2B**) of Zn 2p on Zn-NC-Ti specimens displayed a peak each at 1,044.8 eV (Zn 2p1) and 1,021.8 eV (Zn 2p3), indicating the presence of divalent zinc on the Zn-NC-Ti surfaces.

The CP-Ti surface displayed hydrophobicity with a contact angle of 87.34 ± 0.95, whereas Zn-NC-15, Zn-NC-60, and Zn-NC-120 showed hydrophilicity with the contact angle decreased to 36.23 ± 3.83, 47.81 ± 4.12, and 37.27 ± 4.26, respectively (**Figure 3**). The surface energy of the Zn-NC-Ti samples was significantly higher than that of the CP-Ti specimens, consistent with the trend for hydrophilicity.

Analysis of the concentrations of zinc ions released from Zn-NC-Ti surfaces into PBS (**Figure 4**) showed a continuous

release pattern from the surfaces of the modified samples, with a steady-state zinc ion concentration. In addition, zinc ion released from Zn-NC-15 was higher than that from Zn-NC-60 and Zn-NC-120.

The protein adsorption was significantly higher with Zn-NC-Ti samples than with CP-Ti, consistent with the trend for surface energy (**Figure 5**).

Identification of hMSCs

In order to characterize hMSCs, immunophenotype profiling for specific cell surface antigen sets for hMSCs was measured using flow cytometry. As shown in **Figure 6**, mesenchymal markers including CD29, CD73, and CD105 were positive, and hematopoietic markers including CD34 and CD45 were negative.

Cell Adhesion and Spreading

OBs and hMSCs were cultured on the different surfaces for 1 h, and the cellular nuclei were enumerated (**Figure 7**). Significantly more OBs adhered on the Zn-NC-15 and Zn-NC-120 surfaces than on the CP-Ti and Zn-NC-60 surfaces. All the modified surfaces, especially Zn-NC-15 and Zn-NC-120, exhibited higher attachment of hMSCs than the control surface.

LSCM analysis of the morphology of OBs cultured for 8 h and hMSCs cultured for 24 h on Zn-NC-Ti and CP-Ti surfaces, showed that most of the OBs spread evenly with filopodia; however, cells on the Zn-NC-Ti samples spread better with more outspread pseudopodia than cells on the CP-Ti surface (**Figure 8**). Similarly, hMSCs on CP-Ti showed less elongation than those cultured on Zn-NC-Ti surfaces. The morphology of cells grown on Zn-NC-15, Zn-NC-60, and Zn-NC-120 surfaces was not markedly different.

Cell Proliferation

The proliferation of OBs and hMSCs was determined by the CCK-8 assay (**Figure 9**). The proliferation of OBs on Zn-NC-15 was slightly higher than that on CP-Ti, Zn-NC-60, and Zn-NC-120 after incubation for 1 day. On days 3 and 6, the proliferation of cells cultured on all Zn-NC-Ti samples was significantly higher than that of cells cultured on CP-Ti. The proliferation of hMSCs on days 1 and 3 did not significantly differ. After culturing for 6 days, cell proliferation on Zn-NC-15 and Zn-NC-120 surfaces was significantly higher than that on CP-Ti and Zn-NC-60 surfaces.

ALP Activity

The ALP expression measured by ALP quantitative analysis is shown in **Figure 10**. OBs on Zn-NC-15 surface demonstrated significantly higher ALP activity than the titanium control after 7 days of osteogenic incubation. It could be also observed that Zn-NC-15 and Zn-NC-120 surfaces was apparently higher than that of cells cultured on CP-Ti and Zn-NC-60 surfaces.

Expression of Osteogenesis-Related Proteins

Western blot analysis of the osteogenic differentiation of OBs and hMSCs cultured on the different surfaces (**Figure 11**) revealed that Runx2, OSX, and OCN were upregulated in both cell types cultured on Zn-NC-Ti surfaces compared with the CP-Ti surfaces after 7 days of incubation, with the Zn-NC-15 group showed significant superiority.

Extracellular Matrix Mineralization

After 21 days of osteogenic induction, ECM mineralization was identified by ARS staining of specific calcium-binding sites (**Figure 12**). The ECM mineralization of OBs and hMSCs cultured on the Zn-NC-Ti surfaces was improved than that in the control group. In addition, hMSCs cultured on the Zn-NC-15 surface showed optimal ECM mineralization.

DISCUSSION

Surface treatments for increasing surface roughness, as well as the incorporation of trace elements to make the titanium surface bioactive are responsible for empowering the wettability, bone anchoring, and biomechanical stability between the implant–bone interfaces, thus increasing osteoinduction and osteointegration (Jemat et al., 2015; Contaldo et al., 2021). Various methods have been used to incorporate trace elements into micro/nanostructure modified titanium surfaces (Ming et al., 2017; Shao et al., 2017). Traditional methods of nanostructure preparation included alkali-heat-treatment and acid-alkali-treatment (Pattanayak et al., 2009; Hu and Yang, 2014). The alkali-heat-treatment involves immersion in sodium hydroxide at 60°C for 24 h, incubation in distilled water at 80°C for 24 h, drying in an oven at 60°C for 2 h, and heating to 600°C for 1 h (Ueno et al., 2011). The acid-alkali-treatment involves acid etching followed by hydrothermal alkali-treatment (Yao et al., 2019). However, these techniques are time-consuming or require expensive apparatus. Herein, we explored a modified procedure that quickly and synchronously incorporates zinc and nanostructure on titanium without acid etching or heating and evaluated its effect on surface characteristics and osteocompatibility of OBs and hMSCs. Titanium surfaces were hydrothermally treated with sodium hydroxide followed by a mixed solution of zinc acetate and diammonium hydrogen phosphate, which afforded zinc-incorporated nano-cluster modified titanium surfaces. Zinc acetate is widely used to synthesize zinc-doped nanocomposites with improved antibacterial activity (Amna et al., 2012; Sun et al., 2014), and diammonium hydrogen phosphate has been used in the pretreatment of polyetherimide coatings on magnesium to enhance osteocompatibility and biocorrosion resistance (Yang et al., 2019). In our study, zinc phosphate and acetic acid produced by the mixed solution reacted with the sodium hydroxide -pretreated titanium surface to synchronously incorporate zinc and modify the surface topography at the nanoscale.

As observed by SEM, all Zn-NC-Ti samples showed homogeneous cluster-like nanotopography with differences only in the nanostructure scale. The Zn-NC-15 surface prepared by reaction for 15 min exhibited the smallest nanoscale, whereas the Zn-NC-120 surface appeared thicker deposits. XPS analysis showed that Zn-NC-Ti mainly contained titanium, oxygen, carbon, and zinc, indicating the successful incorporation of zinc into the nano-cluster modified titanium surface. Carbon was mainly present as a surface contaminant (Att et al., 2009; Hori et al., 2010). The contact angle and surface energy histograms showed that all Zn-NC-Ti surfaces, especially the Zn-NC-15 and Zn-NC-120 surfaces, had increased hydrophilicity compared to the

hydrophobic pure titanium. A nanostructure surface has excellent hydrophilicity, which favors cell adhesion, angiogenesis, and osteoinduction (Malhotra and Habibovic, 2016; Teotia et al., 2017). *In vivo* experiments have confirmed that titanium implants with nanoparticulate decorations have high hydrophilicity and accelerate bone formation and osseointegration (Bai et al., 2018).

Zinc ions were rapidly released from the modified titanium surfaces at the initial stage. After 1 day, zinc ions were slowly and continuously released, resulting in a steady zinc ion concentration over time. The role of zinc rich micoenvironments in upregulating the expression of osteogenic genes and eliciting positive biological responses has been confirmed (Park et al., 2018). Moreover, zinc incorporation and the introduction of unique micro-/nano-structures on carbon fiber reinforced polyetheretherketone (CFRPEEK) enhanced cell adhesion, proliferation, and osteo-differentiation (Lu et al., 2016). Accordingly, nanostructure topography, hydrophilicity, and zinc incorporation influence the surface bioactivity of titanium and the osseointegration process, as confirmed by the *in vitro* results of the present study.

When implants are in contact with the physiological environment, water molecules first reach the material surface, followed by protein adsorption, which triggers subsequent cell adhesion and proliferation (Vogler, 2012; Wang et al., 2015). Protein adsorption depends on the surface wettability, which improves the initial host contact (Rupp et al., 2004). As the protein adsorption histogram shown, Zn-NC-Ti surfaces increased protein adsorption, consistent with the trend for hydrophilicity. Supporting our findings, a previous study found improved protein adsorption on nanostructured surfaces due to the rough topography and dynamically increased hydrophilicity (Patelli et al., 2018; Skoog et al., 2018).

The biocompatibility of the synthesized surfaces was evaluated based on their ability to improve adhesion, spreading, proliferation, and differentiation of OBs and hMSCs. The hMSCs in this study were obtained from the alveolar bone by drilling and tapping during implant surgery in a healthy individual. Flow cytometry revealed the high expression of mesenchymal surface markers and scarce expression of hematopoietic surface markers in hMSCs. The results of cell adhesion and spreading indicated that Zn-NC-Ti surfaces promoted early cell attachment and the subsequent spreading of OBs and hMSCs. The interaction between adherent cells and the implant material surface is vital for the induction of physiological functions. A nanoscale topography has been shown to promote cell adhesion, migration, proliferation, and differentiation in various cell types (Nguyen et al., 2016). Nanoscale surfaces quickly and readily increase the detachment force of adherent cells in the initial cell adhesion period within 1 h, consistent with our findings (Naganuma, 2017). Cells adhere to the implant surface through the interaction of integrins on the cytomembrane surface and adhesion proteins on the implant surface (Michael et al., 2009). Therefore, proteins in the culture medium with 10% FBS positively affect cell adhesion on nanostructure surfaces as well (Naganuma, 2017). Zn-NC-15 and Zn-NC-120 exhibited improved cell adhesion and spreading, which can be attributed to their advantageous nanoscale topography and protein adsorption properties. Both OBs and hMSCs adhered to Zn-NC-Ti samples proliferated better than those cultured on CP-Ti after 6 days of incubation. An increase in the number of initial adhered cells on the modified surfaces may have also enhanced the cell proliferation. In addition, zinc-containing microenvironments are reported to promote cell proliferation (Gaffney-Stomberg, 2019; Garino et al., 2019; Wang et al., 2020), which is consistent with our results.

The expression of osteogenesis-related proteins in OBs and hMSCs cultured on the different surfaces was analyzed to evaluate the osteoinduction property of the modified titanium surfaces. ALP, Runx2, Osterix, and OCN are the most commonly studied osteogenic markers during different stages of bone formation. Both Runx2 and Osterix are osteogenic markers with a well-characterized role in the early stage of bone formation (Strecker et al., 2019; Ou and Huang, 2021). OCN, which is involved in ECM deposition, is regarded as a late marker of osteoblast differentiation (Martins et al., 2018). Western blot analysis indicated increased Runx2, Osterix, and OCN expression in OBs and hMSCs, and the expression levels were significantly higher in cells cultured on the Zn-NC-15 surface. The activity of ALP, an early transcription factor, is increased during the differentiation of pre-osteoblasts to osteoblasts (Vimalraj, 2020). Accordingly, the ALP activity of both types of cells cultured on the Zn-NC-15 surface was increased. ECM mineralization occurs in the final stages of osteogenic differentiation. In our ARS staining assay, Zn-NC-Ti markedly increased ECM mineralization after 21 days in OBs and hMSCs compared with that in the control group, with Zn-NC-15 showing the best result in hMSCs. These results suggest that the Zn-NC-Ti surfaces, particularly the surface prepared through the hydrothermal for 15 min, can boost the differentiation of osteoblasts.

We believe that the nano-cluster modification on the titanium surface and the subsequent release of zinc ions together increase the biological activity of the titanium surface, thereby promoting the proliferation, adhesion, and differentiation of OBs and hMSCs. Differences in the biological activity observed between the three Zn-NC-Ti surfaces may be because of differences in their nanoscale topography and zinc release ability. Since Zn-NC-15 showed the most promising results, which also requires the shortest synthesis time, we plan to explore its performance *in vitro* and *in vivo* compared with other titanium surface modifications. Further, the exact mechanism by which this modification promotes bone formation will be investigated.

CONCLUSION

In this study, we established a convenient process to synthesize nano-cluster-modified titanium surfaces with incorporated zinc, without the need for acid etching or heat treatment. Three surfaces were synthesized by varying the reaction time. The surface produced by reaction for 15 min had the best ability to promote the adhesion, proliferation, and osteogenic differentiation of OBs and hBMMSCs. Zn-NC-15 may be further explored for its application to accelerate dental implant osseointegration.

DATA AVAILABILITY STATEMENT

The raw data supporting the conclusions of this article will be made available by the authors, without undue reservation.

AUTHOR CONTRIBUTIONS

Z-HT contributed to design, data acquisition and analysis, and drafted the manuscript. SS, YL, and W-QZ contributed to data acquisition and analysis. S-MZ contributed to design and data analysis. The corresponding author JQ contributed to conception, design, data interpretation, and critically revised the manuscript. All authors give final approval and agree to be accountable for all aspects of the work.

FUNDING

This work was supported by the National Natural Science Foundation of China (Project Number: 81870799), the Jiangsu Provincial Key Research and Development Program (Project Number: BE2019728), the Jiangsu Provincial Medical Youth Talent (Project Number: QNRC2016850), the Nanjing Medical University-SUYAN Group Intelligent Innovation Research and Development Project (Project Number: NMU-SY201806), the Southeast University-Nanjing Medical University Cooperative Research Project (Project Number: 2242017K3DN14), the Science and Technology Development Foundation of Nanjing Medical University (Project Number: NMUB2019072), and the Foundation of Priority Academic Program Development of Jiangsu Higher Education Institutions (Project Number: 2018-87).

SUPPLEMENTARY MATERIAL

The Supplementary Material for this article can be found online at: https://www.frontiersin.org/articles/10.3389/fmats.2021.739071/full#supplementary-material

REFERENCES

Alghamdi, H. S., and Jansen, J. A. (2020). The Development and Future of Dental Implants. *Dent. Mater. J.* 39 (2), 167–172. doi:10.4012/dmj.2019-140

Alvarez, K., Fukuda, M., and Yamamoto, O. (2010). Titanium Implants after Alkali Heating Treatment with a [Zn(OH)4]2− Complex: Analysis of Interfacial Bond Strength Using Push-Out Tests. *Clin. Implant Dent Relat. Res.* 12 (Suppl. 1), e114–e125. doi:10.1111/j.1708-8208.2010.00278.x

Amna, T., Hassan, M. S., Barakat, N. A. M., Pandeya, D. R., Hong, S. T., Khil, M.-S., et al. (2012). Antibacterial Activity and Interaction Mechanism of Electrospun Zinc-Doped Titania Nanofibers. *Appl. Microbiol. Biotechnol.* 93 (2), 743–751. doi:10.1007/s00253-011-3459-0

Att, W., Hori, N., Iwasa, F., Yamada, M., Ueno, T., and Ogawa, T. (2009). The Effect of UV-Photofunctionalization on the Time-Related Bioactivity of Titanium and Chromium-Cobalt Alloys. *Biomaterials* 30 (26), 4268–4276. doi:10.1016/j.biomaterials.2009.04.048

Bai, L., Liu, Y., Du, Z., Weng, Z., Yao, W., Zhang, X., et al. (2018). Differential Effect of Hydroxyapatite Nano-Particle versus Nano-Rod Decorated Titanium Micro-surface on Osseointegration. *Acta Biomater.* 76, 344–358. doi:10.1016/j.actbio.2018.06.023

Brett, P. M., Harle, J., Salih, V., Mihoc, R., Olsen, I., Jones, F. H., et al. (2004). Roughness Response Genes in Osteoblasts. *Bone* 35 (1), 124–133. doi:10.1016/j.bone.2004.03.009

Buser, D., Janner, S. F. M., Wittneben, J.-G., Brägger, U., Ramseier, C. A., and Salvi, G. E. (2012). 10-year Survival and success Rates of 511 Titanium Implants with a Sandblasted and Acid-Etched Surface: a Retrospective Study in 303 Partially Edentulous Patients. *Clin. Implant dentistry Relat. Res.* 14 (6), 839–851. doi:10.1111/j.1708-8208.2012.00456.x

Contaldo, M., De Rosa, A., Nucci, L., Ballini, A., Malacrinò, D., La Noce, M., et al. (2021). Titanium Functionalized with Polylysine Homopolymers: *In Vitro* Enhancement of Cells Growth. *Materials* 14 (13), 3735. doi:10.3390/ma14133735

Gaffney-Stomberg, E. (2019). The Impact of Trace Minerals on Bone Metabolism. *Biol. Trace Elem. Res.* 188 (1), 26–34. doi:10.1007/s12011-018-1583-8

Garino, N., Sanvitale, P., Dumontel, B., Laurenti, M., Colilla, M., Izquierdo-Barba, I., et al. (2019). Zinc Oxide Nanocrystals as a Nanoantibiotic and Osteoinductive Agent. *RSC Adv.* 9 (20), 11312–11321. doi:10.1039/c8ra10236h

Guo, B., Yang, M., Liang, D., Yang, L., Cao, J., and Zhang, L. (2012). Cell Apoptosis Induced by Zinc Deficiency in Osteoblastic MC3T3-E1 Cells via a Mitochondrial-Mediated Pathway. *Mol. Cel Biochem* 361 (1-2), 209–216. doi:10.1007/s11010-011-1105-x

Heberer, S., Kilic, S., Hossamo, J., Raguse, J.-D., and Nelson, K. (2011). Rehabilitation of Irradiated Patients with Modified and Conventional Sandblasted Acid-Etched Implants: Preliminary Results of a Split-Mouth Study. *Clin. Oral Implants Res.* 22 (5), 546–551. doi:10.1111/j.1600-0501.2010.02050.x

Hie, M., Iitsuka, N., Otsuka, T., Nakanishi, A., and Tsukamoto, I. (2011). Zinc Deficiency Decreases Osteoblasts and Osteoclasts Associated with the Reduced Expression of Runx2 and RANK. *Bone* 49 (6), 1152–1159. doi:10.1016/j.bone.2011.08.019

Hori, N., Ueno, T., Suzuki, T., Yamada, M., Att, W., Okada, S., et al. (2010). Ultraviolet Light Treatment for the Restoration of Age-Related Degradation of Titanium Bioactivity. *Int. J. Oral Maxillofac. Implants* 25 (1), 49–62.

Hu, X. N., and Yang, B. C. (2014). Conformation Change of Bovine Serum Albumin Induced by Bioactive Titanium Metals and its Effects on Cell Behaviors. *J. Biomed. Mater. Res.* 102 (4), 1053–1062. doi:10.1002/jbm.a.34768

Jemat, A., Ghazali, M. J., Razali, M., and Otsuka, Y. (2015). Surface Modifications and Their Effects on Titanium Dental Implants. *Biomed. Res. Int.* 2015, 1–11. doi:10.1155/2015/791725

Le Guéhennec, L., Soueidan, A., Layrolle, P., and Amouriq, Y. (2007). Surface Treatments of Titanium Dental Implants for Rapid Osseointegration. *Dental Mater.* 23 (7), 844–854. doi:10.1016/j.dental.2006.06.025

Li, J., Mutreja, I., Tredinnick, S., Jermy, M., Hooper, G. J., and Woodfield, T. B. F. (2020). Hydrodynamic Control of Titania Nanotube Formation on Ti-6Al-4V Alloys Enhances Osteogenic Differentiation of Human Mesenchymal Stromal Cells. *Mater. Sci. Eng. C* 109, 110562. doi:10.1016/j.msec.2019.110562

Lini, F., Poli, P., Beretta, M., Cortinovis, I., and Maiorana, C. (2019). Long-Term Retrospective Observational Cohort Study on the Survival Rate of Stepped-Screw Titanium Implants Followed up to 20 Years. *Int. J. Oral Maxillofac. Implants* 34 (4), 999–1006. doi:10.11607/jomi.7007

Lu, T., Li, J., Qian, S., Cao, H., Ning, C., and Liu, X. (2016). Enhanced Osteogenic and Selective Antibacterial Activities on Micro-/nano-structured Carbon Fiber Reinforced Polyetheretherketone. *J. Mater. Chem. B* 4 (17), 2944–2953. doi:10.1039/c6tb00268d

Malhotra, A., and Habibovic, P. (2016). Calcium Phosphates and Angiogenesis: Implications and Advances for Bone Regeneration. *Trends Biotechnology* 34 (12), 983–992. doi:10.1016/j.tibtech.2016.07.005

Martins, C. M., de Azevedo Queiroz, I. O., Ervolino, E., Cintra, L. T. A., and Gomes-Filho, J. E. (2018). RUNX-2, OPN and OCN Expression Induced by Grey and white mineral Trioxide Aggregate in normal and Hypertensive Rats. *Int. Endod. J.* 51 (6), 641–648. doi:10.1111/iej.12876

Michael, K. E., Dumbauld, D. W., Burns, K. L., Hanks, S. K., and García, A. J. (2009). Focal Adhesion Kinase Modulates Cell Adhesion Strengthening via Integrin Activation. *MBoC* 20 (9), 2508–2519. doi:10.1091/mbc.e08-01-0076

Ming, P.-p., Shao, S.-y., Qiu, J., Yang, J., Yu, Y.-j., Chen, J.-x., et al. (2017). Superiority of Calcium-Containing Nanowires Modified Titanium Surface Compared with SLA Titanium Surface in Biological Behavior of Osteoblasts: A Pilot Study. *Appl. Surf. Sci.* 416, 790–797. doi:10.1016/j.apsusc.2017.04.152

Naganuma, T. (2017). The Relationship between Cell Adhesion Force Activation on Nano/micro-Topographical Surfaces and Temporal Dependence of Cell Morphology. *Nanoscale* 9 (35), 13171–13186. doi:10.1039/c7nr04785a

Nguyen, A. T., Sathe, S. R., and Yim, E. K. F. (2016). From Nano to Micro: Topographical Scale and its Impact on Cell Adhesion, Morphology and Contact Guidance. *J. Phys. Condens. Matter* 28 (18), 183001. doi:10.1088/0953-8984/28/18/183001

Ou, M., and Huang, X. (2021). Influence of Bone Formation by Composite Scaffolds with Different Proportions of Hydroxyapatite and Collagen, official publication of the Academy of Dental Materials. *Dental Mater.* 37, e231–e244. doi:10.1016/j.dental.2020.12.006

Park, K. H., Choi, Y., Yoon, D. S., Lee, K.-M., Kim, D., and Lee, J. W. (2018). Zinc Promotes Osteoblast Differentiation in Human Mesenchymal Stem Cells via Activation of the cAMP-PKA-CREB Signaling Pathway. *Stem Cell Dev.* 27 (16), 1125–1135. doi:10.1089/scd.2018.0023

Patelli, A., Mussano, F., Brun, P., Genova, T., Ambrosi, E., Michieli, N., et al. (2018). Nanoroughness, Surface Chemistry, and Drug Delivery Control by Atmospheric Plasma Jet on Implantable Devices. *ACS Appl. Mater. Inter.* 10 (46), 39512–39523. doi:10.1021/acsami.8b15886

Pattanayak, D. K., Kawai, T., Matsushita, T., Takadama, H., Nakamura, T., and Kokubo, T. (2009). Effect of HCl Concentrations on Apatite-Forming Ability of NaOH-HCl- and Heat-Treated Titanium Metal. *J. Mater. Sci. Mater. Med.* 20 (12), 2401–2411. doi:10.1007/s10856-009-3815-0

Rupp, F., Scheideler, L., Rehbein, D., Axmann, D., and Geis-Gerstorfer, J. (2004). Roughness Induced Dynamic Changes of Wettability of Acid Etched Titanium Implant Modifications. *Biomaterials* 25, 1429–1438. doi:10.1016/j.biomaterials.2003.08.015

Shao, S.-y., Chen, J.-x., Tang, H.-y., Ming, P.-p., Yang, J., Zhu, W.-q., et al. (2020). A Titanium Surface Modified with Zinc-Containing Nanowires: Enhancing Biocompatibility and Antibacterial Property *In Vitro*. *Appl. Surf. Sci.* 515, 146107. doi:10.1016/j.apsusc.2020.146107

Shao, S.-y., Ming, P.-p., Qiu, J., Yu, Y.-j., Yang, J., Chen, J.-x., et al. (2017). Modification of a SLA Titanium Surface with Calcium-Containing Nanosheets and its Effects on Osteoblast Behavior. *RSC Adv.* 7 (11), 6753–6761. doi:10.1039/c6ra26060h

Skoog, S. A., Kumar, G., Narayan, R. J., and Goering, P. L. (2018). Biological Responses to Immobilized Microscale and Nanoscale Surface Topographies. *Pharmacol. Ther.* 182, 33–55. doi:10.1016/j.pharmthera.2017.07.009

Strecker, S. E., Unterman, S., Charles, L. F., Pivovarchick, D., Maye, P. F., Edelman, E. R., et al. (2019). Osterix-mCherry Expression Allows for Early Bone Detection in a Calvarial Defect Model. *Adv. Biosys.* 3 (12), 1900184. doi:10.1002/adbi.201900184

Sun, T., Hao, H., Hao, W.-t., Yi, S.-m., Li, X.-p., and Li, J.-r. (2014). Preparation and Antibacterial Properties of Titanium-Doped ZnO from Different Zinc Salts. *Nanoscale Res. Lett.* 9 (1), 98. doi:10.1186/1556-276x-9-98

Teotia, A. K., Raina, D. B., Singh, C., Sinha, N., Isaksson, H., Tägil, M., et al. (2017). Nano-Hydroxyapatite Bone Substitute Functionalized with Bone Active Molecules for Enhanced Cranial Bone Regeneration. *ACS Appl. Mater. Inter.* 9 (8), 6816–6828. doi:10.1021/acsami.6b14782

Ueno, T., Tsukimura, N., Yamada, M., and Ogawa, T. (2011). Enhanced Bone-Integration Capability of Alkali- and Heat-Treated Nanopolymorphic Titanium in Micro-to-nanoscale Hierarchy. *Biomaterials* 32 (30), 7297–7308. doi:10.1016/j.biomaterials.2011.06.033

Vimalraj, S. (2020). Alkaline Phosphatase: Structure, Expression and its Function in Bone Mineralization. *Gene* 754, 144855. doi:10.1016/j.gene.2020.144855

Vogler, E. A. (2012). Protein Adsorption in Three Dimensions. *Biomaterials* 33 (5), 1201–1237. doi:10.1016/j.biomaterials.2011.10.059

Wang, C., Wang, S., Yang, Y., Jiang, Z., Deng, Y., Song, S., et al. (2018). Bioinspired, Biocompatible and Peptide-Decorated Silk Fibroin Coatings for Enhanced Osteogenesis of Bioinert Implant. *J. Biomater. Sci. Polym. EditionPolymer edition* 29 (13), 1595–1611. doi:10.1080/09205063.2018.1477316

Wang, D., Cui, L., Chang, X., and Guan, D. (2020). Biosynthesis and Characterization of Zinc Oxide Nanoparticles from Artemisia Annua and Investigate Their Effect on Proliferation, Osteogenic Differentiation and Mineralization in Human Osteoblast-like MG-63 Cells. *J. Photochem. Photobiol. B: Biol.* 202, 111652. doi:10.1016/j.jphotobiol.2019.111652

Wang, Y., Deng, H., Huangfu, C., Lu, Z., Wang, X., Zeng, X., et al. (2015). Research of Protein Adsorption on the Different Surface Topography of the Zinc Oxide. *Surf. Interf. Anal.* 47 (2), 245–252. doi:10.1002/sia.5698

Xue, T., Attarilar, S., Liu, S., Liu, J., Song, X., Li, L., et al. (2020). Surface Modification Techniques of Titanium and its Alloys to Functionally Optimize Their Biomedical Properties: Thematic Review. *Front. Bioeng. Biotechnol.* 8, 603072. doi:10.3389/fbioe.2020.603072

Yamaguchi, M. (2010). Role of Nutritional Zinc in the Prevention of Osteoporosis. *Mol. Cel Biochem* 338 (1-2), 241–254. doi:10.1007/s11010-009-0358-0

Yang, Y., Zhou, J., Chen, Q., Detsch, R., Cui, X., Jin, G., et al. (2019). *In Vitro* Osteocompatibility and Enhanced Biocorrosion Resistance of Diammonium Hydrogen Phosphate-Pretreated/Poly(ether Imide) Coatings on Magnesium for Orthopedic Application. *ACS Appl. Mater. Inter.* 11 (33), 29667–29680. doi:10.1021/acsami.9b11073

Yao, Y.-t., Liu, S., Swain, M. V., Zhang, X.-p., Zhao, K., and Jian, Y.-t. (2019). Effects of Acid-Alkali Treatment on Bioactivity and Osteoinduction of Porous Titanium: An *In Vitro* Study. *Mater. Sci. Eng. C* 94, 200–210. doi:10.1016/j.msec.2018.08.056

Yusa, K., Yamamoto, O., Iino, M., Takano, H., Fukuda, M., Qiao, Z., et al. (2016a). Eluted Zinc Ions Stimulate Osteoblast Differentiation and Mineralization in Human Dental Pulp Stem Cells for Bone Tissue Engineering. *Arch. Oral Biol.* 71, 162–169. doi:10.1016/j.archoralbio.2016.07.010

Yusa, K., Yamamoto, O., Takano, H., Fukuda, M., and Iino, M. (2016b). Zinc-modified Titanium Surface Enhances Osteoblast Differentiation of Dental Pulp Stem Cells *In Vitro*. *Sci. Rep.* 6, 29462. doi:10.1038/srep29462

Conflict of Interest: The authors declare that the research was conducted in the absence of any commercial or financial relationships that could be construed as a potential conflict of interest.

Publisher's Note: All claims expressed in this article are solely those of the authors and do not necessarily represent those of their affiliated organizations, or those of the publisher, the editors and the reviewers. Any product that may be evaluated in this article, or claim that may be made by its manufacturer, is not guaranteed or endorsed by the publisher.